Effect of Topology of Water–Ice Mixture on Radar Backscattering by Hailstones

PETR CHÝLEK

Department of Physics and Oceanography, Dalhousie University, Halifax, Nova Scotia, Canada

R. G. PINNICK

Atmospheric Science Laboratory, White Sands Missile Range, New Mexico

V. SRIVASTAVA

Universities Space Research Association, Huntsville, Alabama

(Manuscript received 21 August 1990, in final form 5 December 1990)

ABSTRACT

The radar backscattering cross sections of spongy hailstones are considerably influenced by the topological structure of the water–ice mixture. Observational evidence suggests that such an inhomogeneous composite medium can consist of regions of different topologies. We investigate three different kinds of topologies and derive a general mixed topology mixing rule (MTMR). The mixed topology rule is used to calculate the effective dielectric constant of spongy ice as a function of its liquid-water content. This leads to predictions of backscatter cross sections that are in good agreement with measurement.

1. Introduction

Particles composed of inhomogeneous mixtures of water and ice are frequently present in the atmosphere. Examples are hailstones and melting snowflakes. In both cases a sudden increase in radar reflectivity was observed and related to melting of ice as precipitation particles reached warmer regions of the atmosphere (Ryde 1946; Austin and Bemis 1950; Donaldson 1958, 1961; Atlas and Ludlam 1961).

In general, the interaction of electromagnetic waves with inhomogeneous composite particles comprised of grains smaller than the wavelength is treated by assuming that a composite medium can be characterized by an effective dielectric constant. Many effective medium approximations lack mathematical or physical justification. Their accuracy and range of validity is difficult to establish since there is no exact solution available that can be used for comparison. The literature contains applications of many different "mixing rules," the most widely used being the Bruggeman (1935) and Maxwell-Garnett (1904) rules and volume averaging of refractive indices or dielectric constants.

Early radar meteorologists used an equation attributed to Debye (1929) to calculate the dielectric constant of mixtures of water and ice. Joss (1964) and Atlas et al. (1964) found that calculated backscattering cross sections of spongy ice spheres with dielectric constant given by the Debye formula did not agree with measured cross sections. Later (Bohren and Batten 1980) the use of the Maxwell-Garnett mixing rule was recommended.

In a recent experimental investigation (Chýlek et al. 1988) employing the microwave analog method, it was shown that, in the limit of grain sizes much smaller than the wavelength, the mixing rules of Bruggeman and Maxwell-Garnett (with a proper consideration of which medium forms a matrix and which inclusions) led to phase functions and scattering and extinction cross sections that were in good agreement with measurement. On the other hand, the Maxwell-Garnett mixing rule with the inclusions and matrix materials interchanged, and the volume averaging of refractive indices or dielectric constants led to predictions that strongly disagreed with experimental results. Consequently, we can limit our consideration of the effective medium approach to the dynamic effective medium approximation of Stroud and Pan (1978) of which the Bruggeman and Maxwell-Garnett rules are just two special cases.

2. Effect of topology on dielectric constant of a composite medium

In general, a dielectric constant of a composite material is a function of the dielectric constants of the

Corresponding author address: Petr Chylek, Dept. of Physics, Dalhousie University, Halifax. Nova Scotia B3H 3J5, Canada

components and their respective volume fractions, microstructure, and topology. The microstructure of each component is determined by the shape and size distribution of the grains of that component. The topology can be understood in terms of "connectedness" of individual components.

The dynamic effective medium approximation of Stroud and Pan (1978) is based on the assumption that the spatial averages of electric vector **E** and electric displacement **D** are linearly related, with the proportionality constant being the effective dielectric constant of the composite medium,

$$\langle \mathbf{D} \rangle = \epsilon \langle \mathbf{E} \rangle. \tag{1}$$

Equation (1) defines an effective dielectric constant ϵ of a composite medium and leads to the requirement that the forward scattering amplitude $S(0)$ vanishes when grains are placed in the effective medium (Stroud and Pan 1978).

For simplicity, let us consider a mixture of two materials with dielectric constants ϵ_1 and ϵ_2 and volume fractions f_1 and f_2. There are three basic topologies determined by the way the two components are mixed.

Topology T1 with grains of material ϵ_1 embedded in the continuous matrix of material ϵ_2 is shown in Fig. 1a. Such a mixture has been conventionally modeled by layered spheres with a core of material ϵ_1 and the outside layer of material ϵ_2 (Fig. 1b). In the small grain limit the mixing rule derived from (1) is the Maxwell-Garnett rule (Maxwell-Garnett 1904; Stroud and Pan 1978; Niklasson et al. 1981):

$$\epsilon = \epsilon_2 \frac{(\epsilon_1 + 2\epsilon_2) + 2f_1(\epsilon_1 - \epsilon_2)}{(\epsilon_1 + 2\epsilon_2) - f_1(\epsilon_1 - \epsilon_2)}. \tag{2}$$

Topology T2 represents grains of material ϵ_2 embedded in a continuous matrix of material ϵ_1 (Figs. 1c and d). The small grain limit leads to the Maxwell-Garnett mixing rule of type (2) with ϵ_1 and ϵ_2 interchanged,

$$\epsilon = \epsilon_1 \frac{(\epsilon_2 + 2\epsilon_1) + 2f_2(\epsilon_2 - \epsilon_1)}{(\epsilon_2 + 2\epsilon_1) - f_2(\epsilon_2 - \epsilon_1)}. \tag{3}$$

Aggregate structure topology T3 consists of individual grains of both materials (Fig. 1e). The simplified model is a mixture of spherical particles with dielectric constants ϵ_1 and ϵ_2 (Fig. 1f) imbedded in the effective medium. The small grain limit leads to the Bruggeman (1935) rule,

$$f_1 \frac{\epsilon_1 - \epsilon}{\epsilon_1 + 2\epsilon} + f_2 \frac{\epsilon_2 - \epsilon}{\epsilon_2 + 2\epsilon} = 0. \tag{4}$$

The important difference between the topologies T1 and T2 is that in T1 it is the material with a dielectric constant ϵ_2, which is interconnected throughout the composite particle, while in the T2 case the material with ϵ_1 is interconnected.

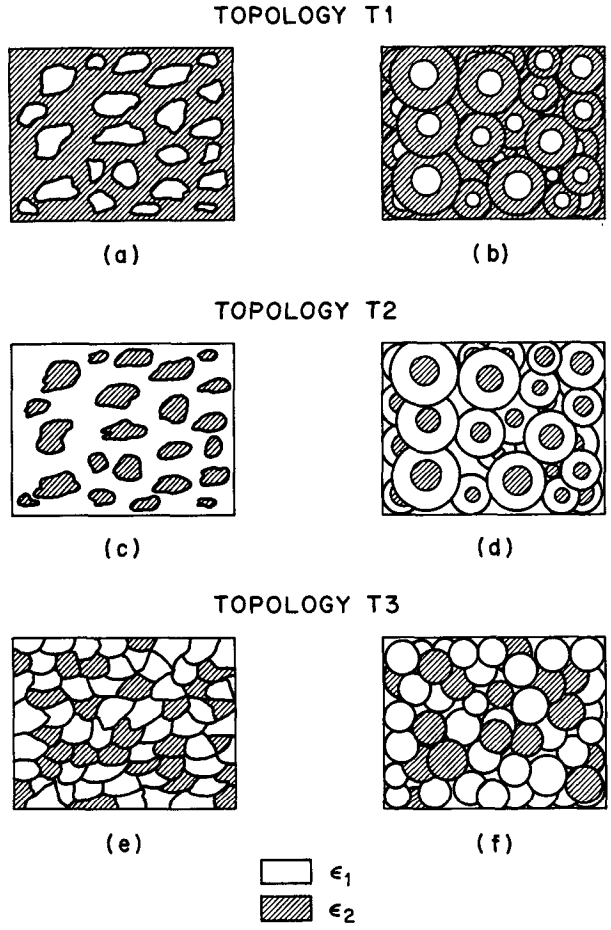

FIG. 1. Schematic representation of the two-component mixed structure. (a) Topology T1 leading to the Maxwell-Garnett mixing rule with component of dielectric constant ϵ_1 embedded in a continuous matrix of dielectric constant ϵ_2. (b) Layered sphere model of (a). (c) Topology T2 leading to the Maxwell-Garnett mixing rule with component of dielectric constant ϵ_2 embedded in a matrix of dielectric constant ϵ_1. (d) Layered sphere model of (c). (e) Aggregate structure topology T3 leading to the Bruggeman mixing rule with two components distributed randomly. (f) Homogeneous sphere model of (e).

The effect of connectedness is illustrated in Fig. 2, which shows, for different topologies, the imaginary part of the effective dielectric constant of the water–ice mixture as a function of the liquid-water fraction. The Maxwell-Garnett rule with ice grains surrounded by a connected water matrix (MGT1) leads to a much higher imaginary part of ϵ than the (inverted) Maxwell-Garnett rule for disconnected water droplets surrounded by an ice matrix (MGT2). In the case of aggregate structure topology T3 (BRT3), the component with a small volume fracture is usually disconnected. In general, different regions of the composite medium may have different topologies. Let V_1, V_2, and V_3 represent volume fractions of a composite medium with types of topology T1, T2, and T3. In the small grain

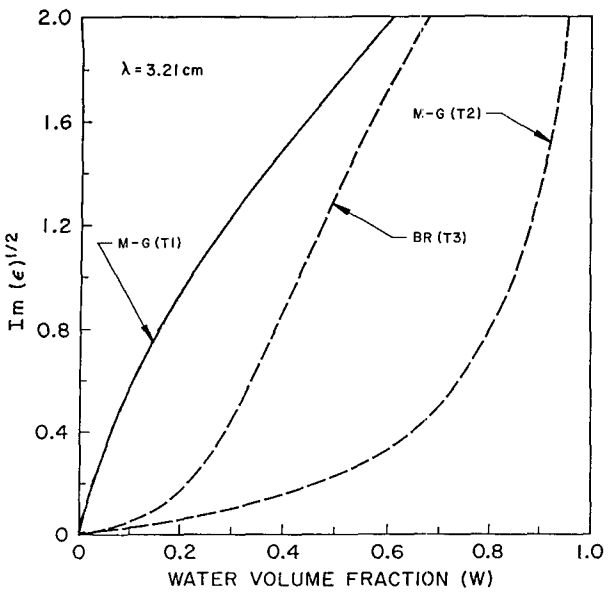

FIG. 2. Imaginary part of the effective refractive index of water–ice mixture $\mathrm{Im}(\epsilon)^{1/2}$ as a function of volume fraction W of water for the wavelength 3.21 cm. The highest refractive index and absorption is generally obtained for a continuous water matrix (Maxwell-Garnett topology T1) and the least absorption for water pockets embedded in an ice matrix (Maxwell-Garnett topology T2). In the case of Bruggeman topology T3, water is in the form of isolated water pockets at low volume fraction leading to low absorption; at higher volume fractions water forms connected chains leading to high absorption.

limit, (1) leads to the following mixed topology mixing rule (MTMR),

$$V_1 \frac{(\epsilon_2 - \epsilon)(\epsilon_1 + 2\epsilon_2) + f_1(2\epsilon_2 + \epsilon)(\epsilon_1 - \epsilon_2)}{(\epsilon_2 + 2\epsilon)(\epsilon_1 + 2\epsilon_2) + 2f_1(\epsilon_2 - \epsilon)(\epsilon_1 - \epsilon_2)} + V_2 \frac{(\epsilon_1 - \epsilon)(\epsilon_2 + 2\epsilon_1) + f_2(2\epsilon_1 + \epsilon)(\epsilon_2 - \epsilon_1)}{(\epsilon_1 + 2\epsilon)(\epsilon_2 + 2\epsilon_1) + 2f_2(\epsilon_1 - \epsilon)(\epsilon_2 - \epsilon_1)} + V_3\left(f_1 \frac{\epsilon_1 - \epsilon}{\epsilon_1 + 2\epsilon} + f_2 \frac{\epsilon_2 - \epsilon}{\epsilon_2 + 2\epsilon}\right) = 0$$

$$\text{with } V_1 + V_2 + V_3 = 1 \text{ and } f_1 + f_2 = 1. \quad (5)$$

When only one type of topology is present, the mixed topology mixing rule (5) reduces to one of the previously listed Maxwell-Garnett or Bruggeman rules: (2), (3), or (4).

3. Topological structure of the water–ice mixture in hailstones

To determine the topological structure of the water–ice mixture we have studied (Chýlek et al. 1984) a large number of photographs of thin sections of quenched hailstones collected by Knight and Knight (1968, 1973). The most common form of spongy hail appears to be a graupel soaked with water. The water is confined in connected cellular veins and sheets that are intertwined with a connected ice matrix (Fig. 3). At low liquid-water fractions some of the water veins and sheets are partially frozen and part of the water is confined to several disconnected regions. Thus the process of freezing leads to a gradual change in water–ice topology. Some of the originally connected water veins are gradually split into many disconnected segments, and at very low liquid-water fractions most of the remaining water will be in the form of isolated water pockets surrounded by a continuous ice structure. This observation is in general agreement with results of other investigators (Prodi et al. 1980, 1986a, and 1986b). Therefore, the topology of the water–ice mixture is a function of liquid-water content. We have a connected water matrix at very high liquid-water content (which can be modeled by a Bruggeman mixing rule or a Maxwell-Garnett mixing rule with a continuous water matrix) and disconnected water segments at very low water fractions. In between both water and ice are in the form of connected intertwined structures.

To model analytically this transition from one topology to another we assume somehow arbitrarily that the transition from connected water structure into disconnected water segments starts at the liquid-water fraction around 0.2, and that the volume of the region with a still connected water matrix decreases from this point linearly to zero with the decreasing liquid-water content. The chosen value of 0.2 is within the range of between 0.15 and 0.30 suggested for the threshold of complete connectedness by percolation theory results

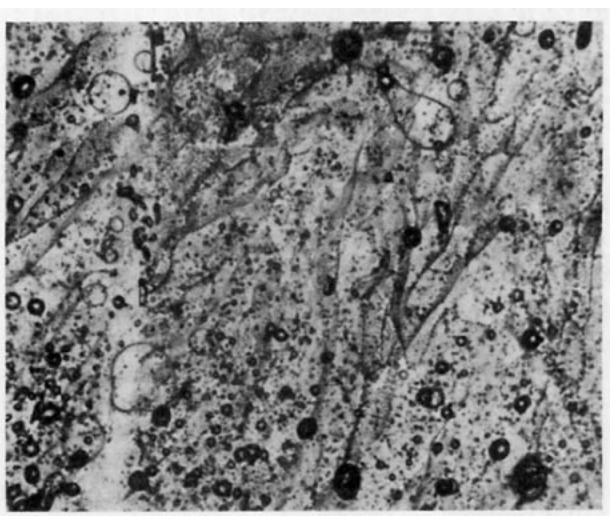

FIG. 3. Magnified portion of quenched graupel shows water component in the water–ice mixture as gray areas, suggesting connectedness of water in high water-content regions. Regions of low water concentration (which appear mostly white) suggest that water also exists in disconnected pockets. Complex hailstone structure may have more than one type of topology. Photograph by C. A. Knight and N. C. Knight, taken from Chýlek et al. (1984).

(Wood and Ashcroft 1977). The value of 0.2 was chosen for simplicity and not to fit any particular dataset. We have verified that our results and conclusions are not dependent on the exact value of this parameter within the 0.1 and 0.5 range.

One of possible simple models of the described liquid-water–dependent topology is the mixed topology mixing rule with a connected water matrix for liquid-water fractions $W > 0.2$ (topology T1) and the coexisting connected intertwined water and ice structures for $W < 0.2$ (mixture of topologies T1 and T2). The appropriate mixed topology mixing rule can be obtained as a special case of the general rule (5):

$$5W\frac{\begin{matrix}(\epsilon_W-\epsilon)(\epsilon_I+2\epsilon_W)\\ +(1-W)(2\epsilon_W+\epsilon)(\epsilon_I-\epsilon_W)\end{matrix}}{\begin{matrix}(\epsilon_W+2\epsilon)(\epsilon_I+2\epsilon_W)\\ +2(1-W)(\epsilon_W-\epsilon)(\epsilon_I-\epsilon_W)\end{matrix}} + (1-5W)\frac{\begin{matrix}(\epsilon_I-\epsilon)(\epsilon_W+2\epsilon_I)\\ +W(2\epsilon_I+\epsilon)(\epsilon_W-\epsilon_I)\end{matrix}}{\begin{matrix}(\epsilon_I+2\epsilon)(\epsilon_W+2\epsilon_I)\\ +2W(2\epsilon_I-\epsilon)(\epsilon_W-\epsilon_I)\end{matrix}} = 0 \quad (6a)$$

for $0 < W < 0.2$, and

$$\epsilon = \epsilon_W = \frac{(\epsilon_I+2\epsilon_W)+2(1-W)(\epsilon_I-\epsilon_W)}{(\epsilon_I+2\epsilon_W)-(1-W)(\epsilon_I-\epsilon_W)} \quad (6b)$$

for $W > 0.2$, where ϵ_I and ϵ_W are dielectric constants of ice and liquid water and ϵ is the dielectric constant of the water–ice mixture. The behavior of the imaginary part of ϵ in this case of mixed topology is shown in Fig. 4 for the wavelength = 3.21 cm. If we chose liquid-water content $W = 0.5$ (instead of 0.2) as the limit above which all water is within a connected structure, the factors $5W$ and $(1 - 5W)$ in (6a) are replaced by $2W$ and $(1 - 2W)$, respectively, and (6b) remains unchanged.

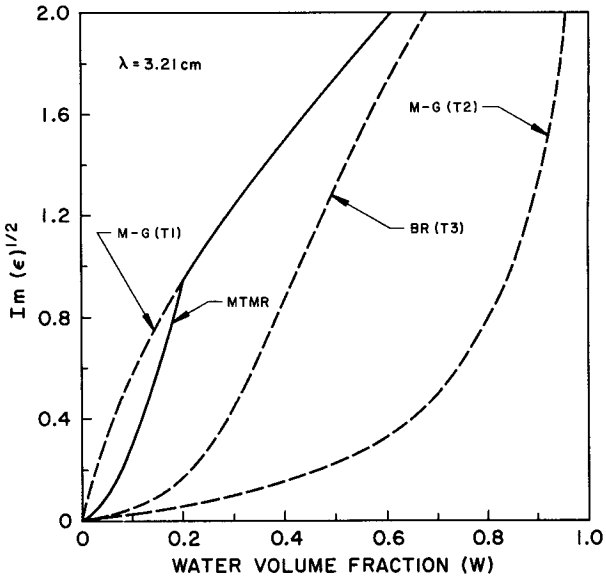

FIG. 4. Calculations of imaginary part of effective refractive index $\mathrm{Im}(\epsilon)^{1/2}$ of water–ice mixture, for wavelength 3.21 cm, using mixed topology (solid line). For reference the results for individual topologies are also shown.

4. Comparison with experimental results

Joss and Aufdermaur (1965) measured the backscattering cross sections of individual spongy ice spheres as a function of liquid-water content. Figure 5 shows the measured normalized backscattering cross section of a sphere as a function of time at the wavelengths 3.21 cm, 4.67 cm, and 10 cm. The sphere, which initially consisted of an ice core surrounded by a shell of spongy ice, was exposed to subfreezing temperatures. The fraction of water in the shell decreased with time until, at the 5.2-min mark, all of the water was frozen. Joss and Aufdermaur (1965) assumed that the water fraction changed linearly with time from an initially known value of 40% to 0% in 5.2 min. However their results as shown on Fig. 5 are completely independent of this assumption. The linear transition between the water and ice volumes would affect only the scale of the horizontal axis of Fig. 5 if one would try to relabel this axis with liquid-water content (instead of time) as an independent variable. Since it is not quite clear that the transition has to be linear we prefer to keep time as an independent variable of the Joss Aufdermaur (1965) measurements.

For numerical calculations we use the layered sphere model (Bohren and Huffman 1980) with the core composed of ice and the outer layer composed of the water–ice mixture. The only new feature introduced in our work is the means by which an effective refractive index of the water–ice mixture is calculated. In Bohren and Battan (1980) the Bruggeman expression for a dielectric constant (4) is called the effective medium dielectric constant.

Results of our numerical calculation using the mixed topology mixing rule (MTMR) as given by (6a) and (6b) are shown in Fig. 6a. There is overall good agreement between experimental and theoretical results at all three wavelengths (3.21, 4.67, and 10 cm), including the crossover points.

For comparison, the results obtained using the Bruggeman and Maxwell-Garnett (for ice grains in water matrix) rules are shown in Figs. 6b,c. The Bruggeman rule shows a dip at about 20% water fraction at the wavelength 4.67 cm, which is not observed experimentally. In addition the dip below 10% liquid-water content at $\lambda = 3.21$ cm is too deep as compared with measurements (Fig. 5). The Maxwell-Garnett rule also does not reproduce the experimentally observed intersection of backscattering cross sections at wavelengths 3.21 and 10 cm below 10% liquid-water fraction.

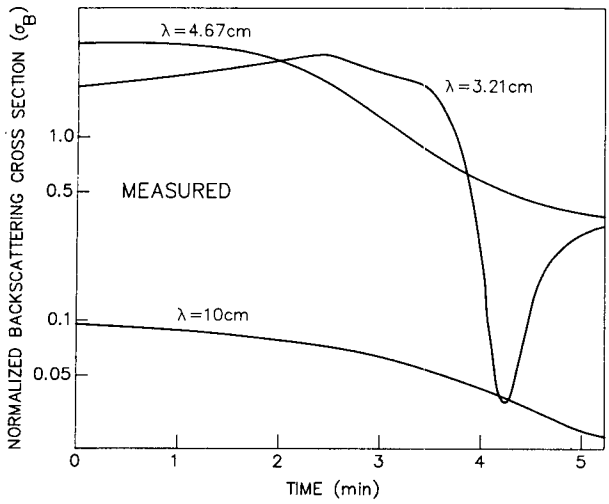

FIG. 5. Measured normalized backscattering cross section σ_B of spongy ice sphere (radius = 0.68 cm, shell thickness = 0.26 cm) as a function of time at wavelengths 3.21, 4.67, and 10 cms. All the water in the stone is assumed to be frozen after about 5.2 min. Taken from Joss and Aufdermaur (1965).

By comparing calculated results of Fig. 6 with the laboratory measurements of Fig. 5, it is apparent that the mixed topology mixing rule given by formulas (6a and 6b) leads to numerical results, which are in better agreement with experiment than either the Bruggeman or Maxwell-Garnett rules.

By considering a spongy ice as a two component water–ice mixture, we are neglecting possible effects of air bubbles. Their presence in water or in snow would mean that the refractive indices of water and ice would have to be replaced by effective refractive indices of water–air and ice–air mixtures. Since the refractive index of air bubbles is close to 1, a small amount of air bubbles would not change significantly the obtained results.

5. Effect of shape of grains on a dielectric constant of a composite medium

The effect of replacing spherical grains by ellipsoidal ones in the Maxwell-Garnett rule was investigated by Bohren and Battan (1982). The effective dielectric constant ϵ of the mixture is given by

$$\epsilon = \frac{W\epsilon_W - (1-W)B\epsilon_I}{W + (1-W)B} \tag{7}$$

where

$$B = \frac{2\epsilon_W}{\epsilon_I - \epsilon_W}\left(\frac{\epsilon_I}{\epsilon_I - \epsilon_W}\log\frac{\epsilon_I}{\epsilon_W} - 1\right).$$

Similarly, the Bruggeman mixing rule for ellipsoidal grains averaged over all possible shapes and orientations is given by Pinnick et al. (1985):

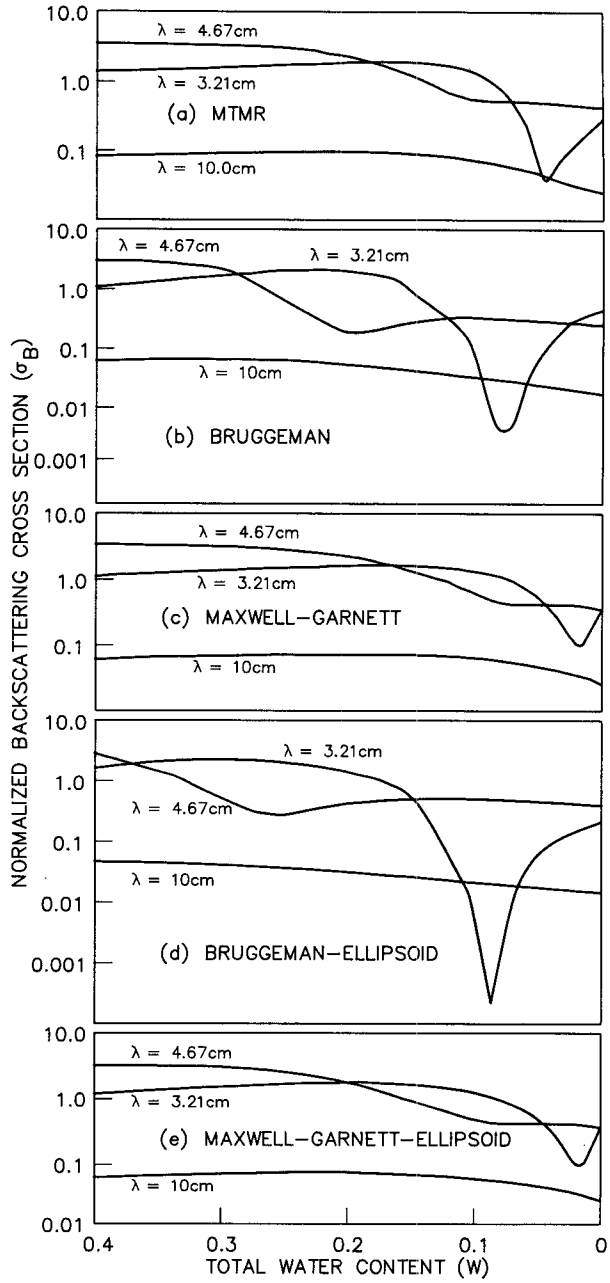

FIG. 6. (a) Calculated normalized backscattering cross section σ_B as a function of total water content W using mixed topology. The mixed topology mixing rule for water–ice mixture leads to good agreement with measurements of Joss and Aufdermaur (Fig. 5). (b) Calculated normalized backscattering cross sections as a function of total water content W in the spongy ice sphere (as described in Fig. 5) for wavelengths λ = 10, 4.67, and 3.21 cm using Bruggeman mixing rule and (c) Maxwell-Garnett mixing rule for ice grains in water matrix. None of the calculations adequately reproduce the measurements of Fig. 5. Ellipsoidal grains [(d) and (e)] do not produce any improvement.

$$\frac{2(1-W)\epsilon}{\epsilon_I-\epsilon}\left(\frac{\epsilon_I}{\epsilon_I-\epsilon}\ln\frac{\epsilon_I}{\epsilon}-1\right)+\frac{2W\epsilon}{\epsilon_W-\epsilon}\left(\frac{2\epsilon_W}{\epsilon_W-\epsilon}\ln\frac{\epsilon_W}{\epsilon}-1\right)=1. \quad (8)$$

This equation can be solved by an iterative method using the effective dielectric constant obtained from the Bruggeman rule (4) as an initial guess. Numerical results using the ellipsoidal shape mixing rules (7) and (8) are shown in Figs. 6e, f. No improvement of the fit between measurements and calculation is achieved. For the case of the Maxwell-Garnett mixing rule, a similar conclusion was reached by Bohren and Battan (1982).

6. Conclusion

There is experimental evidence that the topology of the water–ice mixture in hailstones changes with the amount of liquid water present. To account for this change of topology we have derived the general mixed topology mixing rule (5) using the dynamic effective medium approximation of Stroud and Pan (1978). For applications to spongy hail we have proposed to use a simplified form of this rule in the form of (6a) and (6b). Although we have used the liquid-water fraction of 0.2 as a transition point between different topologies the numerical results are not affected significantly with change of this transition point between 0.1 and 0.5.

Comparison of numerical calculations with laboratory measurements of Joss and Aufdermaur (1965) shows that the mixed topology mixing rule leads to better agreement between calculated and measured backscattering cross sections than any of the other mixing rules considered.

There is obviously a need for additional experimental measurements under the controlled laboratory conditions to provide an additional dataset that can serve for comparison of theoretical and experimental results and provide additional information concerning the topology of water–ice mixture.

Acknowledgments. Part of the reported research was accomplished while the first author was visiting the Physics Department of the New Mexico State University in Las Cruces, NM. This research was supported in part by the U.S. Army Research Office (Grant DAAL03-K-0093), Atmospheric Environment Service, and Natural Sciences and Engineering Research Council of Canada.

REFERENCES

Atlas, D., and F. H. Ludlam, 1961: Multiwavelength radar re-reflectivity of hailstones. *Quart. J. Roy. Meteor. Soc.*, **87**, 523–534.

——, K. R. Hardy and J. Joss, 1964: Radar reflectivity of storms containing spongy hail. *J. Geophys. Res.*, **69**, 1955–1961.

Austin, P. M., and A. C. Bemis, 1950: A quantitative study of the "bright band" in radar precipitation echoes. *J. Meteor.*, **7**, 145–151.

Bohren, C. F., and L. J. Battan, 1980: Radar backscattering by inhomogeneous precipitation particles. *J. Atmos. Sci.*, **37**, 1821–1827.

——, and ——, 1982: Radar backscattering of microwaves by spongy ice spheres. *J. Atmos. Sci.*, **39**, 2623–2628.

Bruggeman, D. A. G., 1935: Berechnung verschiedener Physikalischer Konstanten von heterogenen Substanzen. I: Dielektrizitatskonstanten und Leifahigkeiten del Mischkorper aus isotropen Substanzen. *Ann. Phys. (Leipzig)*, **24**, 636–679.

Chýlek, P., B. R. D. Gupta, N. C. Knight and C. A. Knight, 1984b: Distribution of water in hailstones. *J. Climate Appl. Meteor.*, **23**, 1469–1472.

——, V. Srivastava, R. G. Pinnick and R. T. Wang, 1988: Scattering of electromagnetic waves by composite spherical particles: Experiment and effective medium approximations. *Appl. Opt.*, **27**, 2396–2404.

Debye, P., 1929: *Polar Molecules.* The Chemical Catalog Company.

Donaldson, R. J. Jr., 1958: Analysis of severe convective storms observed by radar. *J. Meteor.*, **15**, 44–50.

——, 1961: Radar reflectivity profiles in thunderstorms. *J. Meteor.*, **18**, 292–305.

Joss, J. 1964: Die Bestimmung der Ruckstruequerschnitte von Eis-Wasser Gemischen bei einer Wellenlange. von 5.05 cm. Z. *Angew. Math. Phys.*, **15**, 509–539.

——, and A. N. Aufdermaur, 1965: Experimental determination of radar cross sections of artificial hailstones containing water. *J. Appl. Meteor.*, **4**, 723–726.

Knight, C. A., and N. C. Knight, 1968: The final freezing of spongy ice: Hailstone collection technique and interpretation of structures. *J. Appl. Meteor.*, **7**, 875–881.

——, and ——, 1973: Quenched spongy hail. *J. Atmos. Sci.*, **30**, 1665–1671.

Maxwell-Garnett, J. C., 1904: Colors in metal glasses and in metallic films. *Phil Trans. Roy. Soc. London*, **A203**, 385–420.

Niklasson, G. A., C. G. Granqvist and O. Hunderi, 1981: Effective medium models for the optical properties of inhomogeneous materials. *Appl. Opt.*, **20**, 26–30.

Pinnick, R. G., S. G. Jennings, D. C. Boice and J. R. Cruncleton, 1985: Attenuated total reflectance measurements of the complex refractive index of Kaolinite powder at CO_2 laser wavelengths. *Appl. Opt.*, **24**, 3274–3285.

Prodi, F., C. T. Nagamoto and J. Rosinski, 1980: A preliminary study of ice grown by droplet accretion using water insoluble particles as tracers. *J. Appl. Meteor.*, **10**, 284–289.

——, G. Santachiara and A. Franzini, 1986a: Properties of ice accreted in two-stage growth. *Quart. J. Roy. Meteor. Soc.*, **112**, 1057–1080.

——, L. Levi and P. Pederzoli, 1985b: The density of accreted ice. *Quart. J. Roy. Meteor. Soc.*, **112**, 1081–1090.

Ryde, J. W., 1946: The attenuation and radar echoes produced at centimeter wavelengths by various meteorological phenomena, in meteorological factors in radio wave propagation. *Phys. Soc., London*, 169–188.

Stroud, D., and F. D. Pan, 1978: Self-consistent approach to electromagnetic wave propagation in composite media: Application to model granular metals. *Phys. Rev.*, **B17**, 1602–1610.

Wood, D. M., and N. W. Ashcroft, 1977: Effective medium theory of optical properties of small particle composites. *Philos. Mag.*, **35**, 269–280.